APPLICATIONS

1. *Multiple Sclerosis*
2. *Brain Tumor*
3. *MR Angiography*
4. *Kinematic Analysis of Joints*
5. *Quantification of Mammographic Density and Multimodal Breast Image Registration*
6. *CT Colonography*
7. *Upper Airway Disorders in Children*
8. *CT Angiography*
9. *Digital Topological Analysis of Trabecular Bone using in vivo Micro MRI*
10. *Lung Ventilation/Perfusion via MRI and CT*

APPLICATIONS

1. Multiple Sclerosis

To study the natural course of this disease via imaging and to determine its response to therapy. The ultimate goal is to develop an MRI-based quantitative scale in place of the present subjective score scale which is based on neuro-cognitive and motor tests.

We use multiple MRI protocols including T2, PD, T1, T1 with Gd, MT, and MR spectroscopy.

The images are segmented for different tissue regions (WM, GM, CSF, lesions, diseased WM, normal WM).

Various quantitative parameters are estimated from each protocol image in each tissue region.

Images are registered among the various protocols so that complementary information from different protocols can be ascertained and compared.

Tests are conducted to determine which parameters and which protocols produce the most disease-specific information.

Over 1,500 studies performed.

Team: J.K. Udupa, D.C. Hackney, T. Lei, L. Balcer, R. Doty, and D. Kolson.

Brain Segmentation, MS Lesion Quantification

FSE T2 (A) and FSE PD (B) images of a MS patient. The GM (C), WM (D), CSF (E), and LS (F) objects segmented as 3D fuzzy connected objects are shown in the slices. A close up of one of the lesions (G) and its fuzzy segmentation (H) are also shown to emphasize the fuzzy nature of the lesion.

(a) (b) (c) (d)

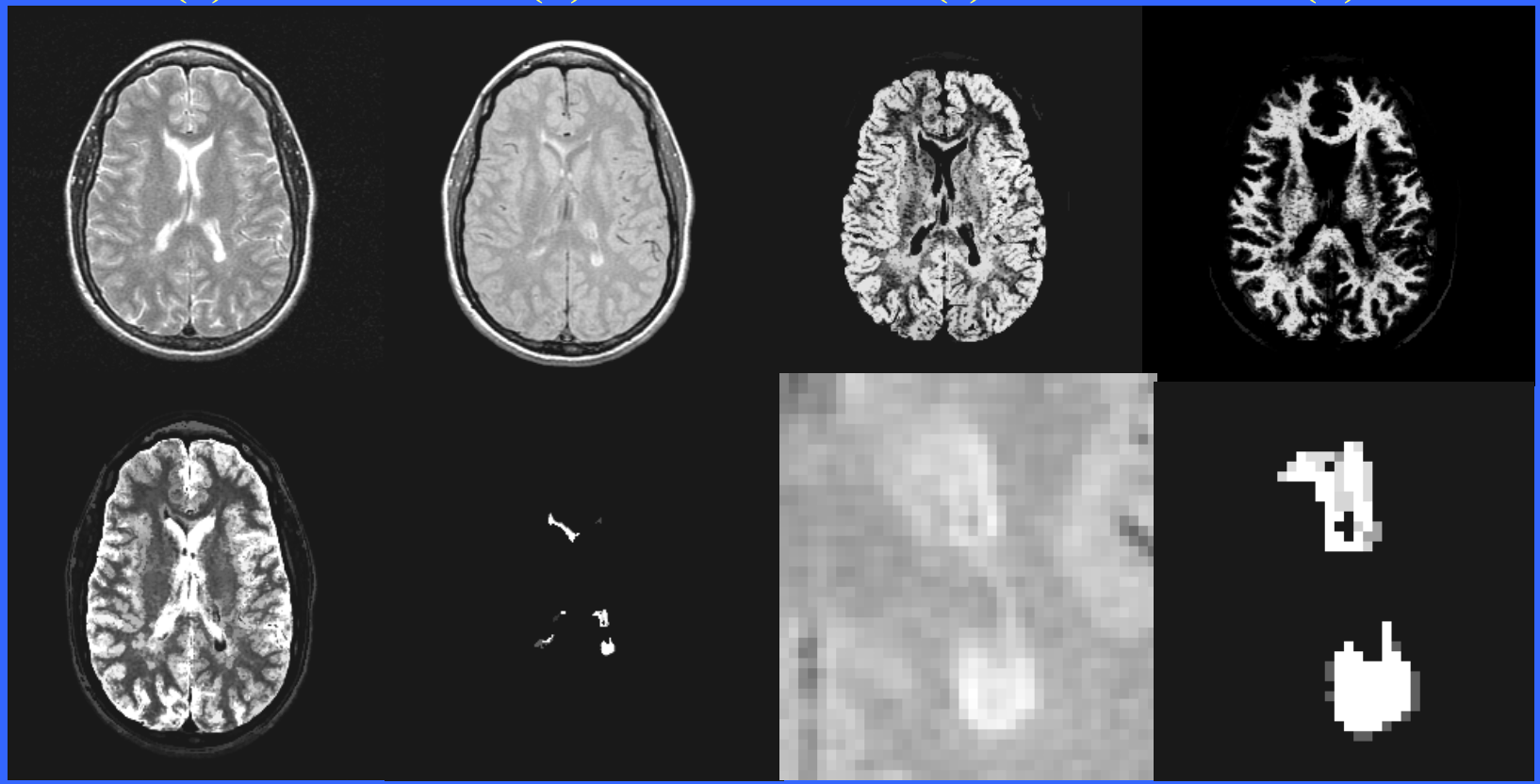

(e) (f) (g) (h)

2. Brain Tumor

To accurately and precisely determine tumor volumetrics for staging disease and for assessing the effect of therapy.

We use multiple MRI protocols including, FLAIR, T1, T1 with Gd in multiple acquisitions.

Tumor is segmented in FLAIR, T1, T1 with Gd and in (T1-T1 with Gd) images. Volume of edema and enhancing tumor is computed.

By studying standardized MRI intensities in longitudinal acquisitions in the vicinity of tumor regions, we are studying if tumor growth can be predicted.

Over 50 studies done.

Team: D.C. Hackney, J.K. Udupa, J.G. Liu, and G. Moonis.

Flair

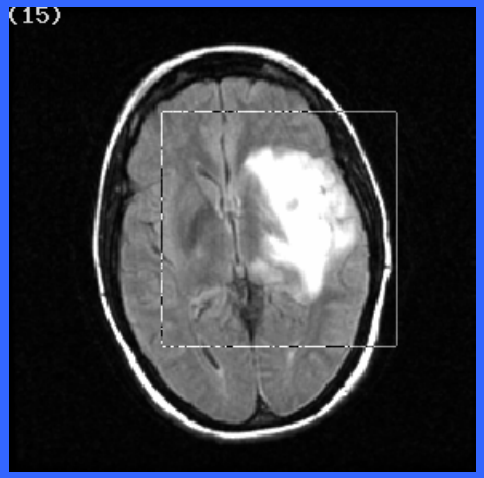

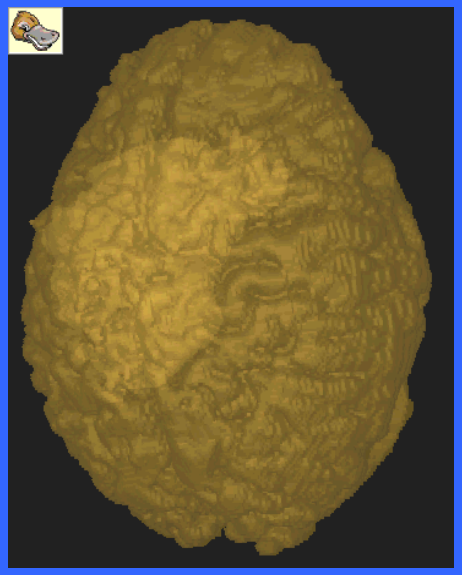

Edema +
Brain (SR)

T1

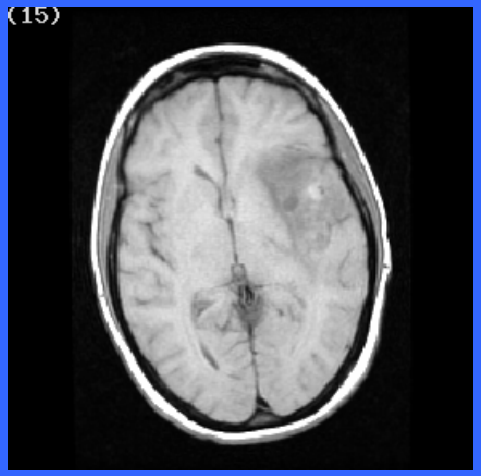

Enhancing tumor +
brain (SR)

T1E

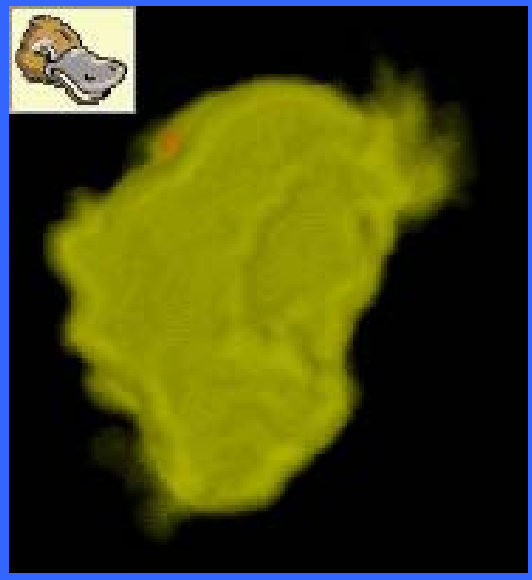

Edema + enhancing
tumor (VR)

3. MR Angiography

To clearly display the vascular tree free of other clutters and to visualize arteries and veins independently via contrast-enhanced MRA.

Arteries and veins are separated via segmentation. A software package has been developed specially for this purpose.

Over 150 studies done successfully.

Team: J.K. Udupa, T. Lei, and EPIX Medicals, Inc.

(a)

(b)

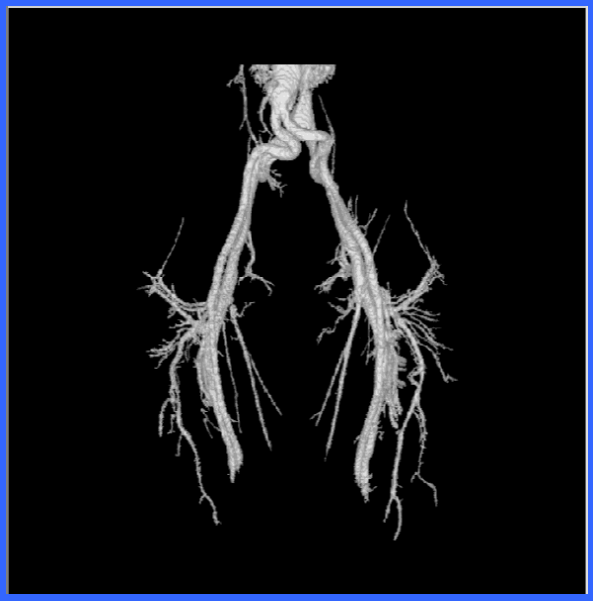

(c)

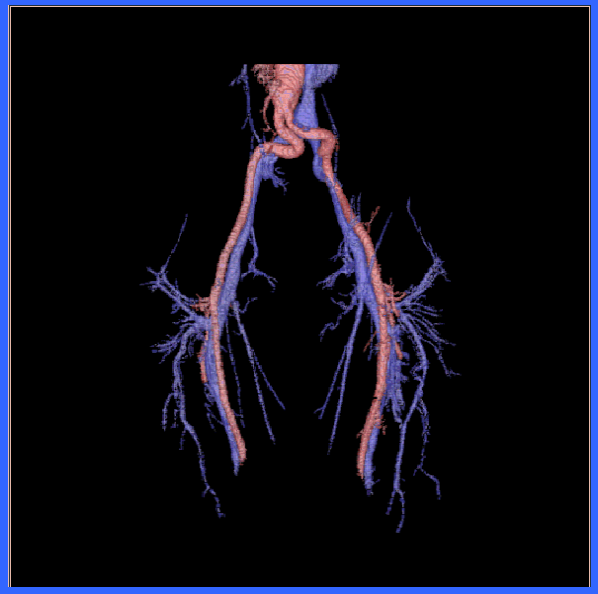

(d)

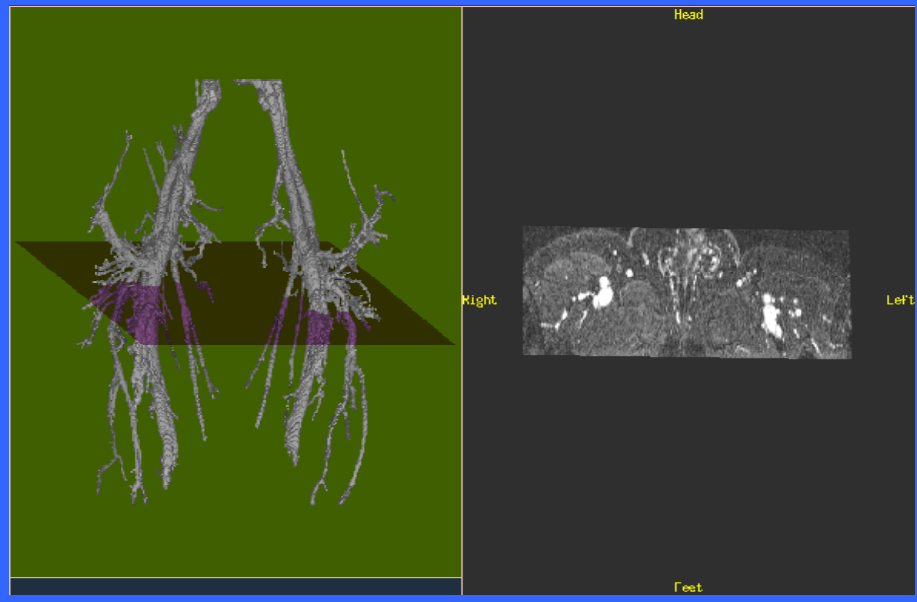

Artery/Vein Separation: (a) MIP rendition of an original MRA image, (b) Segmented vessel image, (c) Separated artery (red) and vein (blue) images, (d) "Seed" point selections.

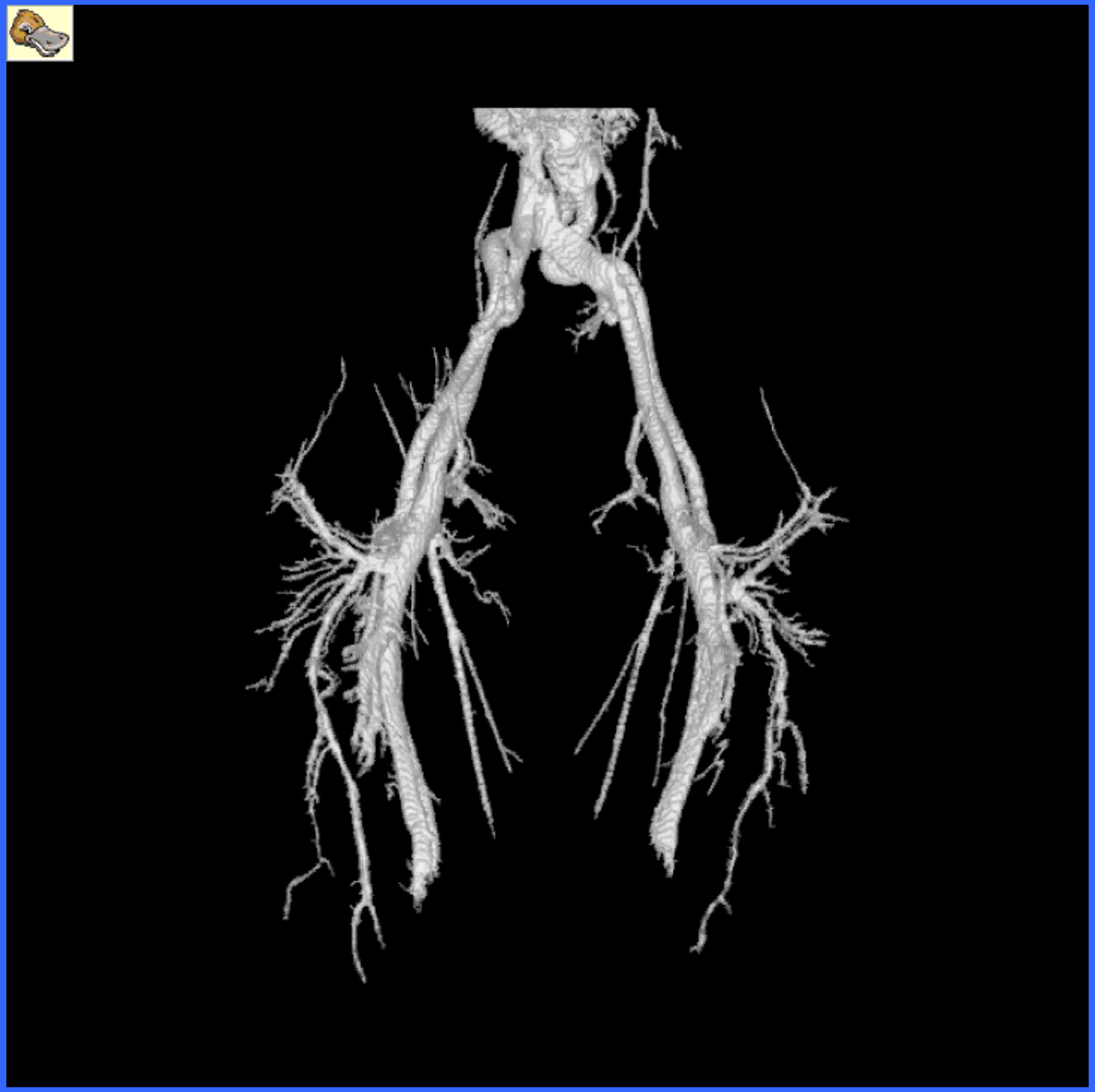

4. Kinematic Analysis of Joints

To understand the normal morphology, architecture, and kinematics of the bones at a joint via MRI and to identify, classify, and quantify deviations due to pathologies including ligament injuries, architectural abnormalities, and arthritis.

To assess effects of surgery and compare objectively surgery procedures.

MR images are acquired for different positions of the joint, the bones are segmented, and rigid motions are estimated.

Over 80 studies (normal and pathological) done involving the shoulder joint and the mid tarsal joints of the foot and cervical spine.

Team: J.K. Udupa, S. Siegler, B.E. Hirsch, J. Liu, P.K. Saha, E. Okereke, S. Simon, B. Winkelstein, and J. Woodburn.

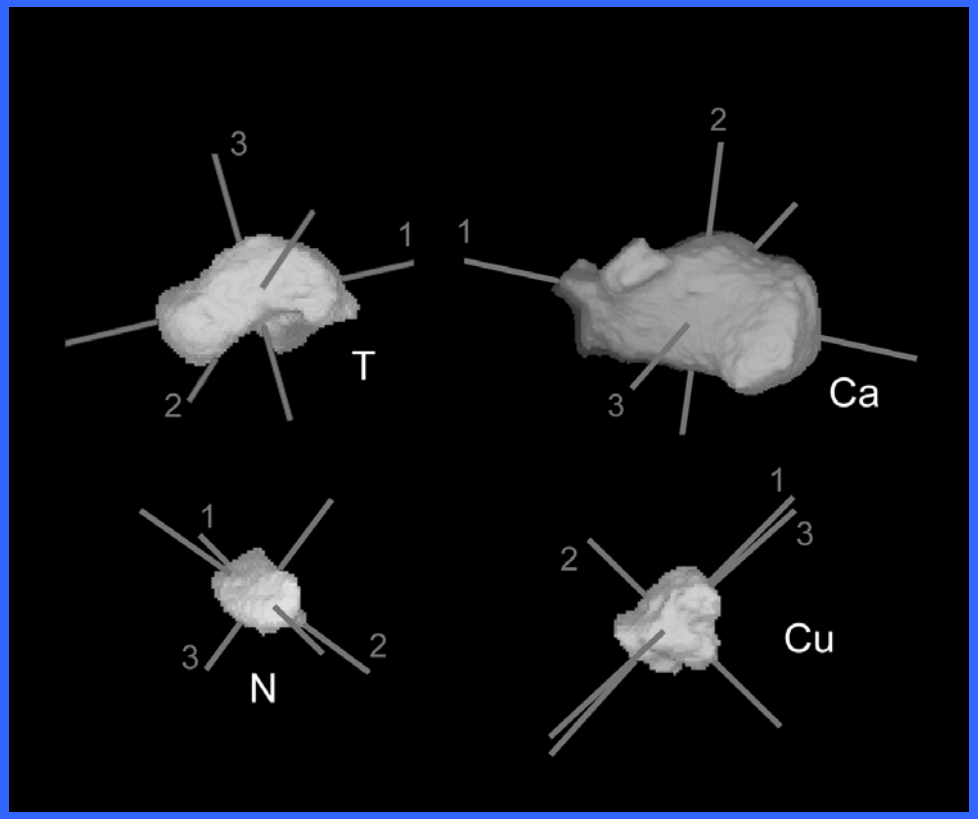

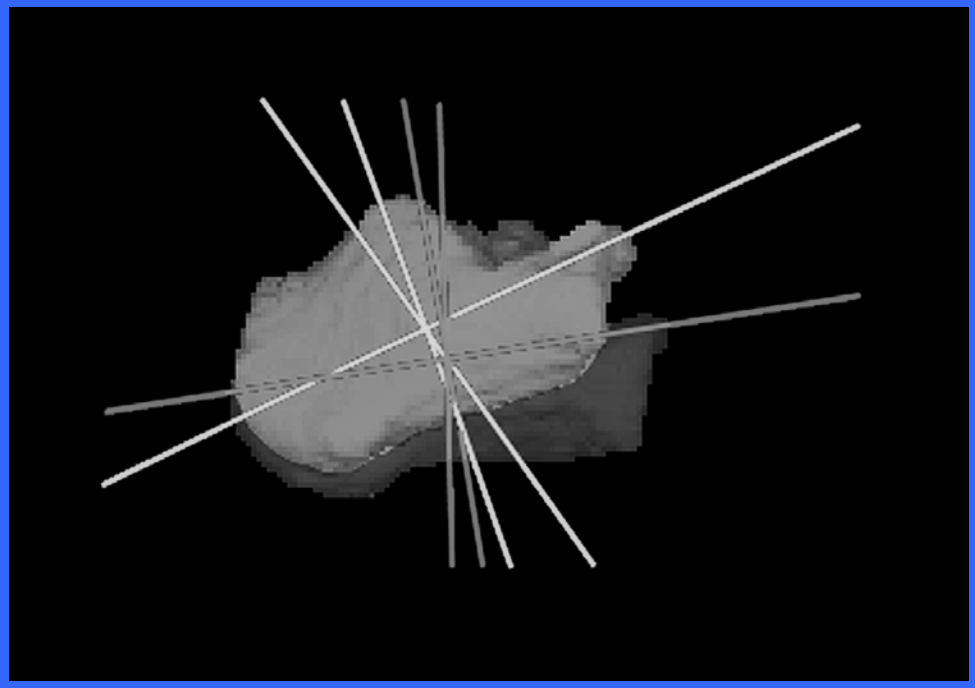

To measure the motion of the irregularly shaped foot bones, it is necessary to mathematically determine a set of unique, intersecting, mutually perpendicular lines which represent each bone. These lines are called the principal axes. These are the principal axes for the calcaneus, talus, navicular, and cuboid of normal foot.

A calcaneus and its associated principal axes are shown in two positions. It is possible to measure the amount of motion, both rotatory and linear, which the bone undergoes as it moves.

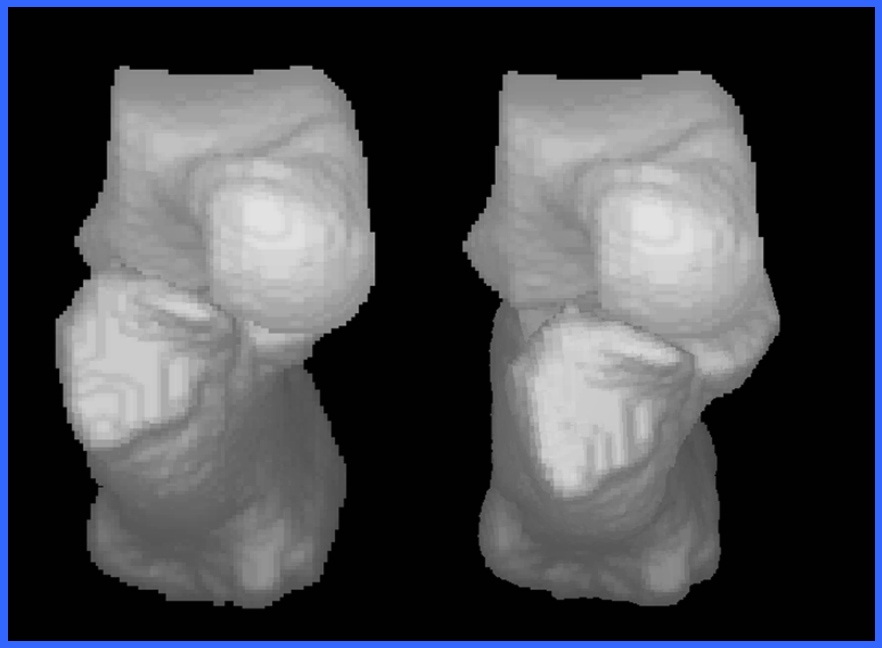

The talus (ankle bone) and calcaneus (heel bone) of a foot in two positions. Motion is shown in such a way that the talus appears not to move.

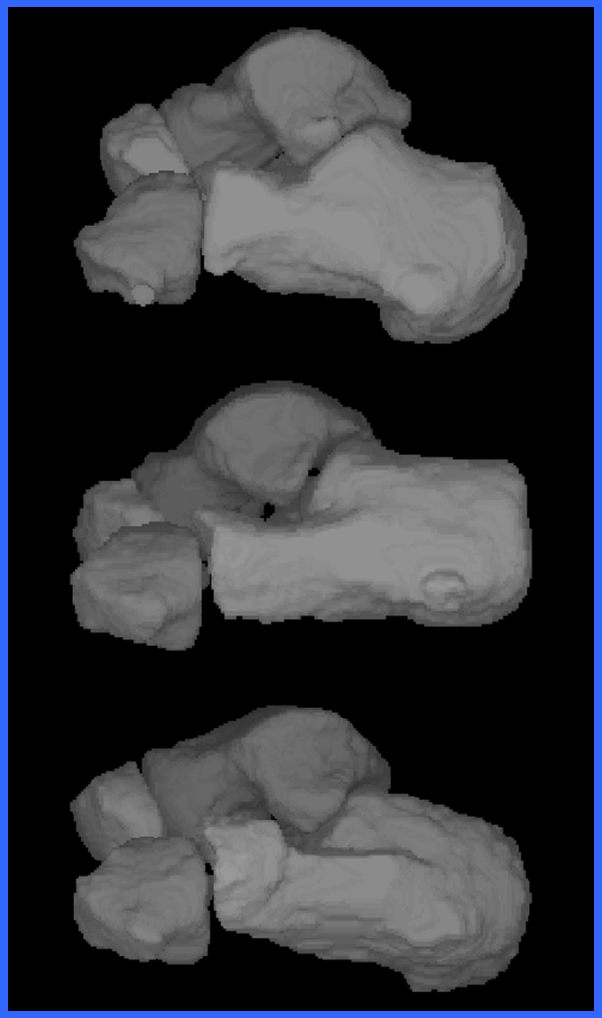

Side views of the rear of a normal foot (top), compared to the same region of a boy with a congenital flat foot (middle). After surgery (bottom), the form of the foot is almost normal.

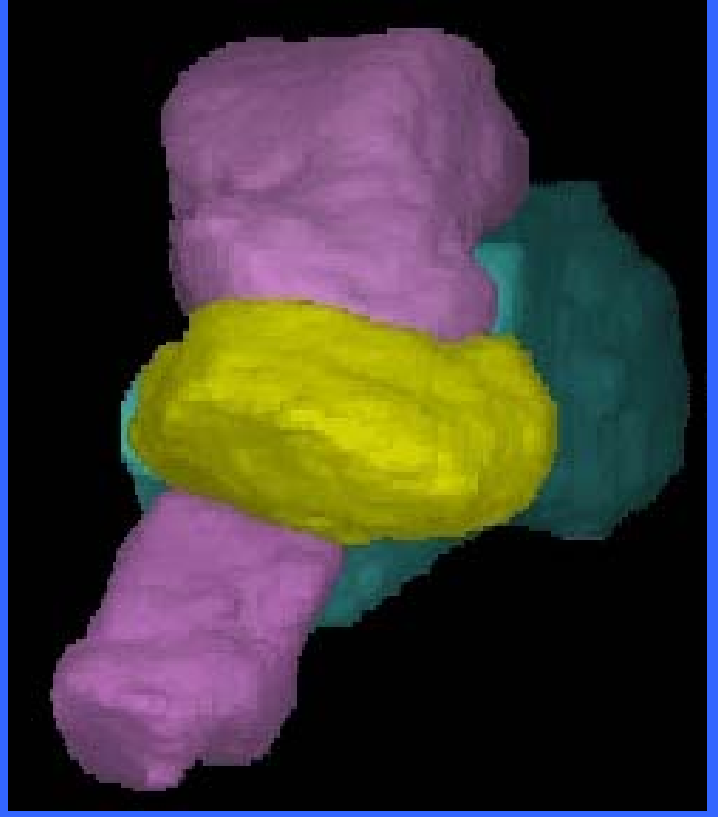

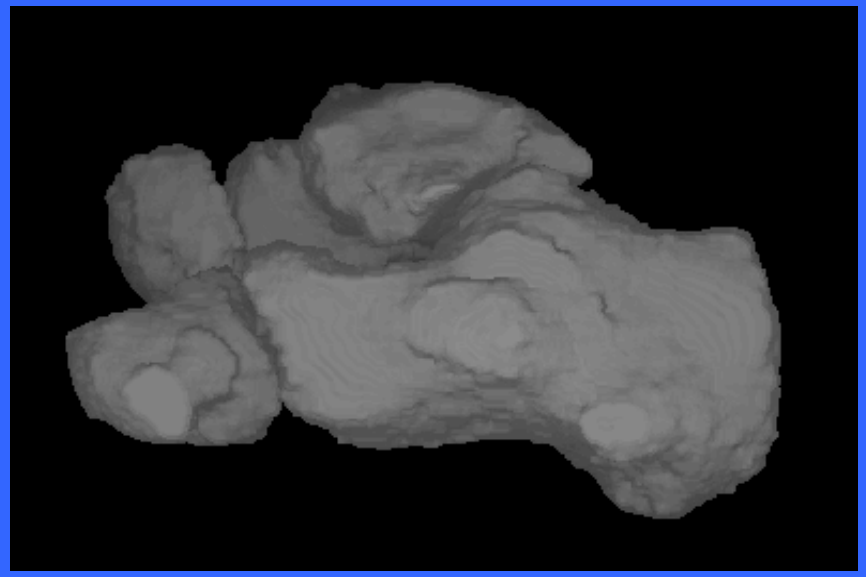

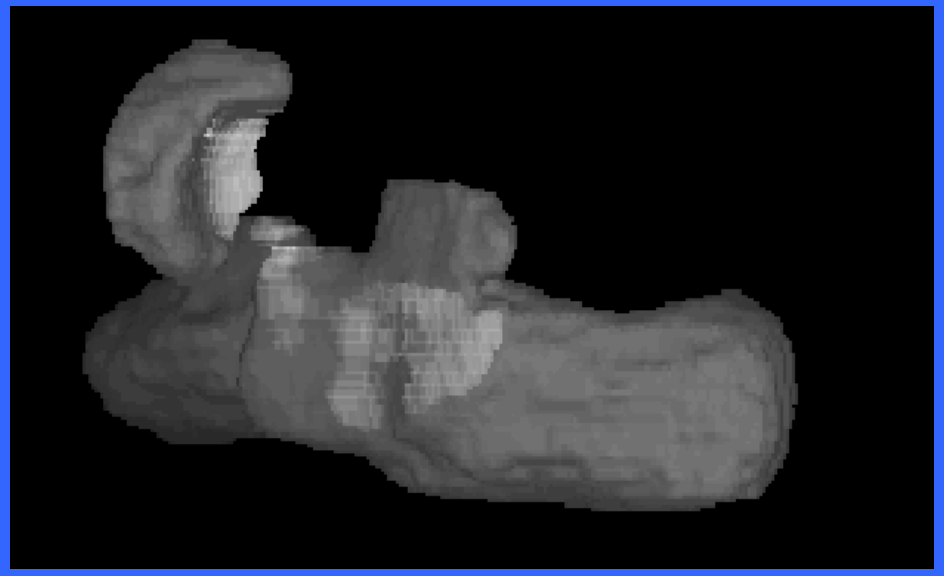

A lateral view of the bones of the rearfoot.

The light areas show the contact areas of the talus against the calcaneus and the navicular.

5. Quantification of Mammographic Density and Multimodal Breast Image Registration

To quantify the density of breast via digitized mammograms. Dense breasts are known to be at higher risk for cancer than less dense breasts. The method is automatic and produces very similar density values for the same breast in mammograms taken at different angles. Density quantification is useful for managing patients, for determining effects of therapies (such as hormone) on breast density.

We are developing methods to register breast images obtained via mammography, digital mammography, US, PET, and MRI to investigate how the multimodality information may be utilized to improve the detection of breast cancer.

Team: J.K. Udupa, P.K. Saha, G.J. Grevera, E. Conant, A. Blackwood, and M. Schnall.

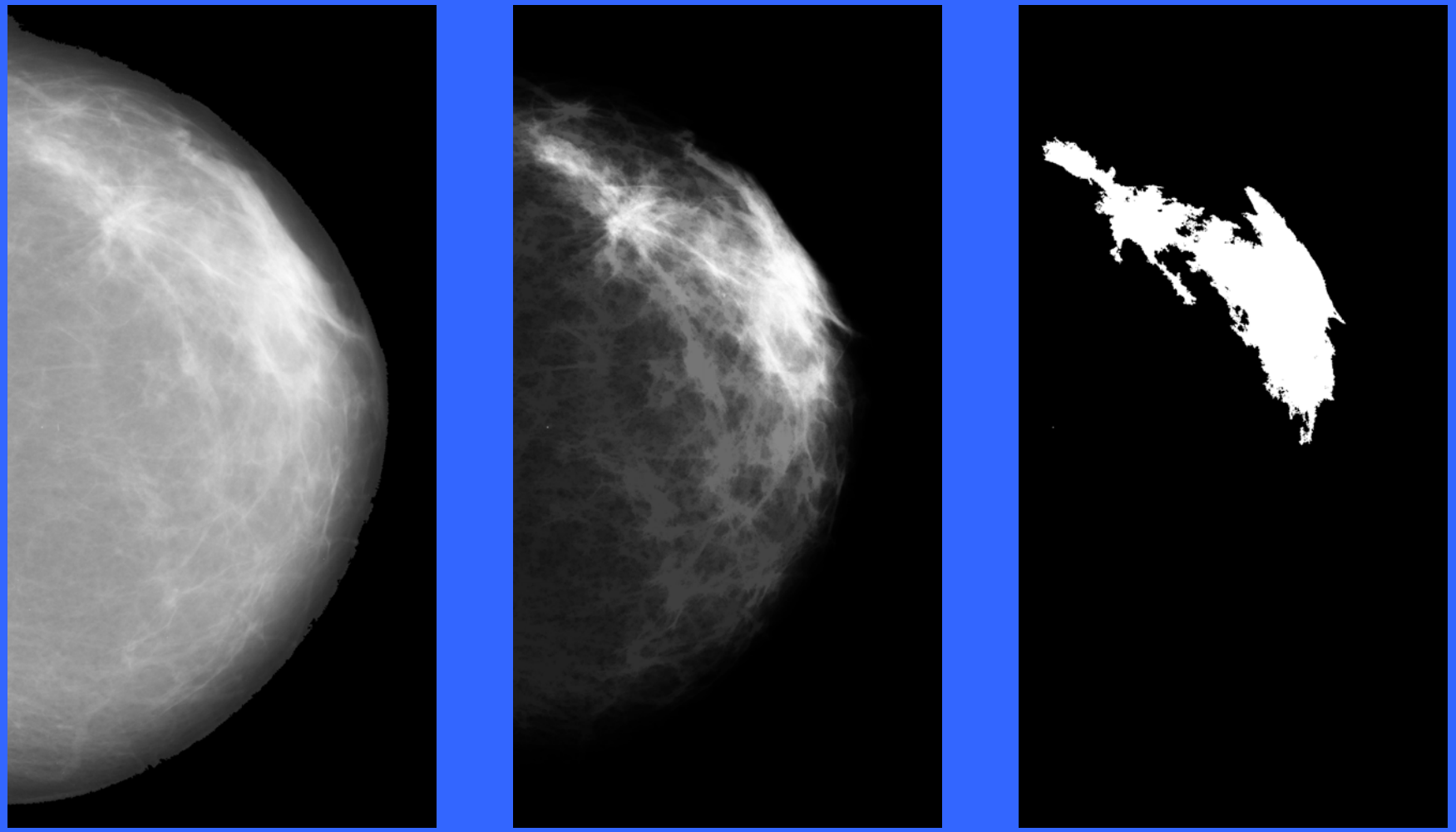

(a) (b) (c)

Quantification of Mammographic Density: (a) Original mammogram, (b) Fuzzy connectedness scene for dense regions, (c) Segmented dense region. Measured parameters — Area of Density (AD) 1.09×10^5 (in # of pixels), AD/Area of Breast (AB) 0.11, Total Density (TD) 2.16×10^8, TD/AB 217.63.

Registration Using Markers

- Digital Mammography
- MRI
- Ultrasound
- PET

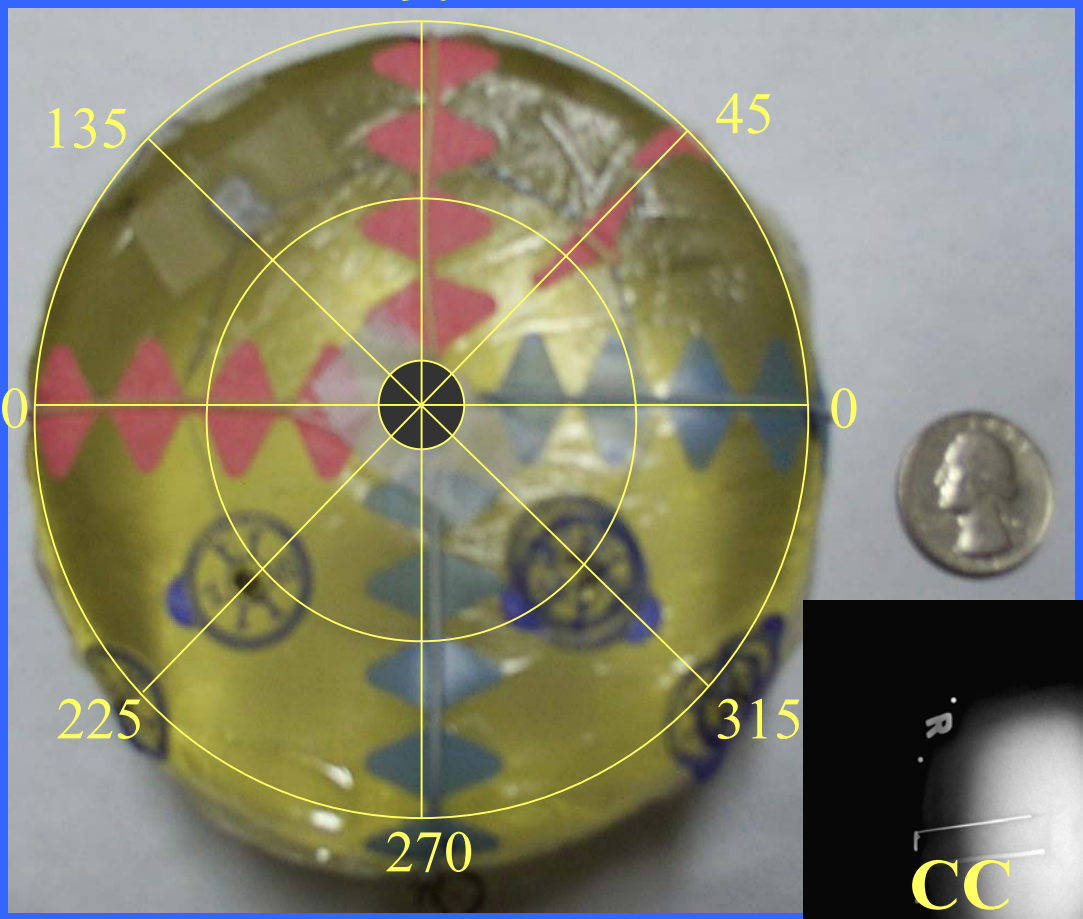

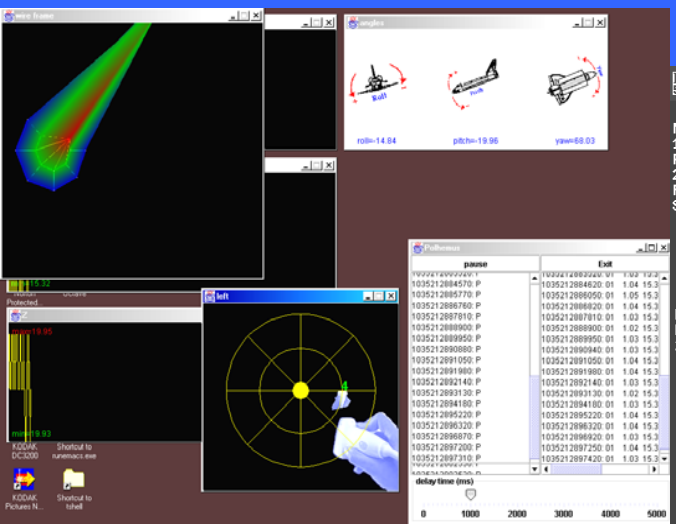

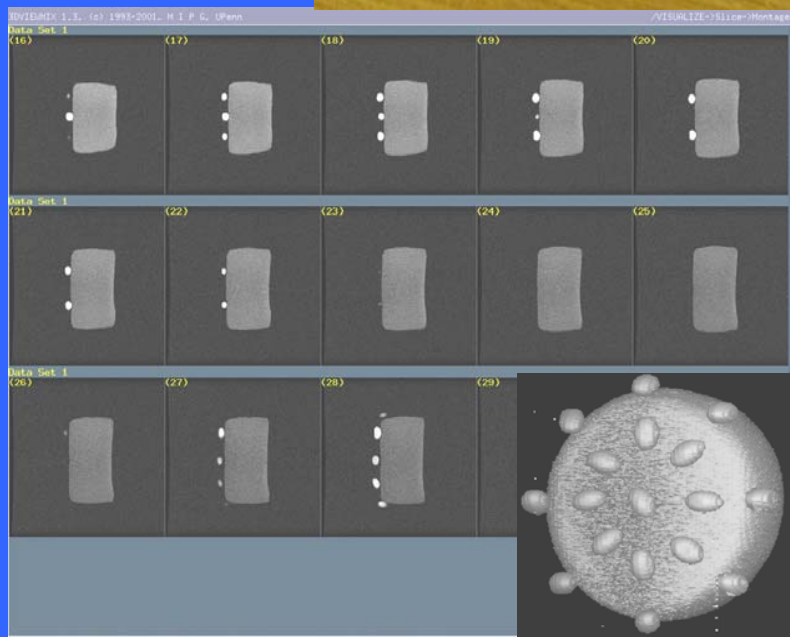

6. CT Colonography

To facilitate colon examination using CT without the discomfort of the conventional colonoscoy.

The method we developed is different from other available methods in that it does not miss any part of the colon and it uses fuzzy connectedness instead of thresholding for colon segmentation.

The method uses the central line of the colon for guiding viewing and shell rendering.

Team: J.K. Udupa, D. Odhner, and H. Eisenberg.

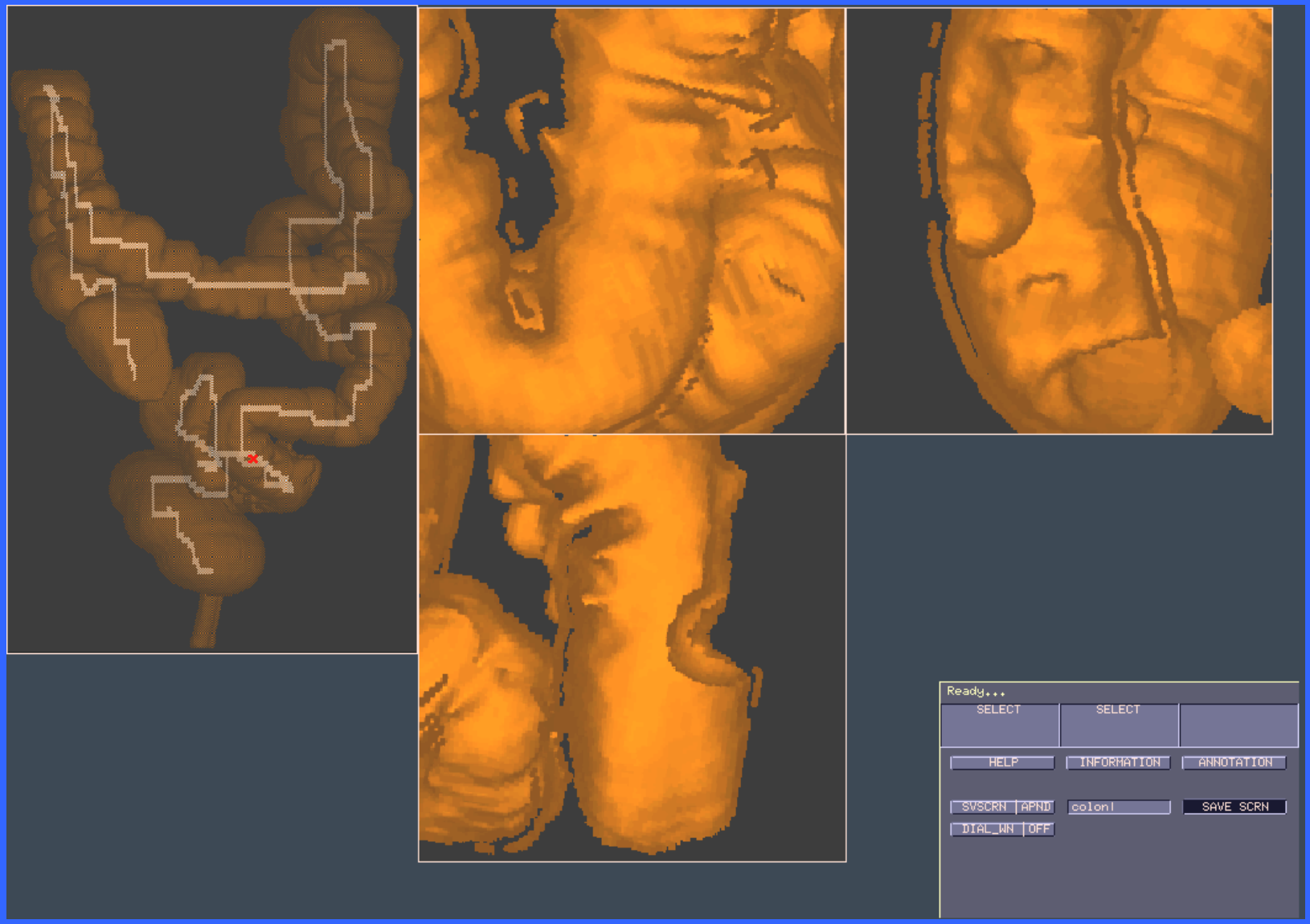

CT Colonography: (a) A rendition of the whole colon of a patient with the central line through the colon. (b), (c), (d): The three en-face views for the viewpoint indicated by *x* in (a). The three views have some overlap, but cover all aspects of the colon seen from the viewpoint all around. Movies of the three views are generated as the viewpoint moves along the central line in real time.

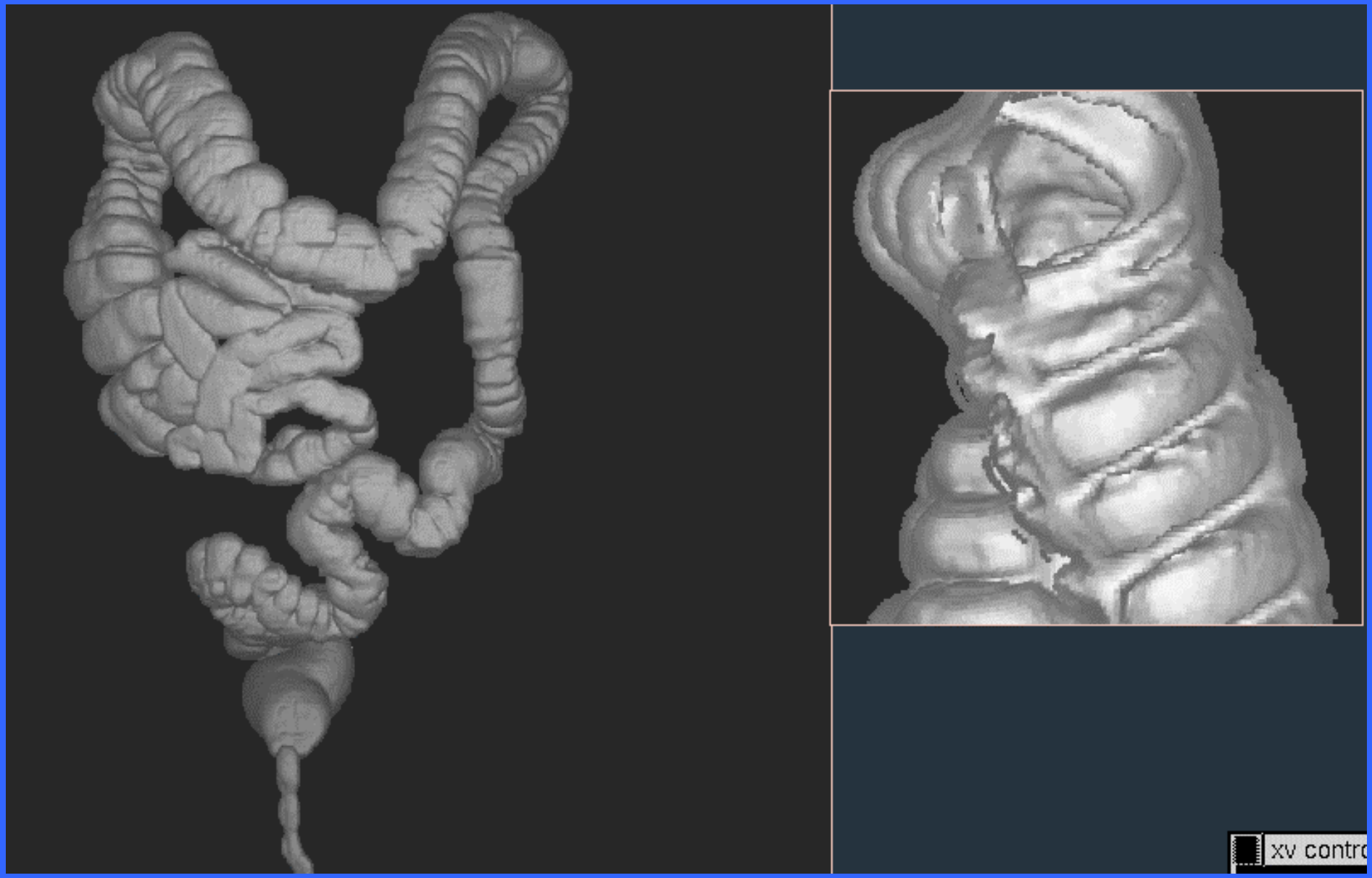
xv contro

7. Upper Airway Disorders in Children

To develop image analysis and visualization techniques for understanding how the structure of the airway and the architecture of the surrounding soft tissue organs influence upper airway disorders in children.

Multiprotocol MR images are used including T1, T2, PD and T1 with Gd.

Various structural and morphological parameters are utilized in characterizing normal groups and in distinguishing them from pathological.

Team: R. Arens, J. McDonough, J.K. Udupa, J.G. Liu, and D. Odhner.

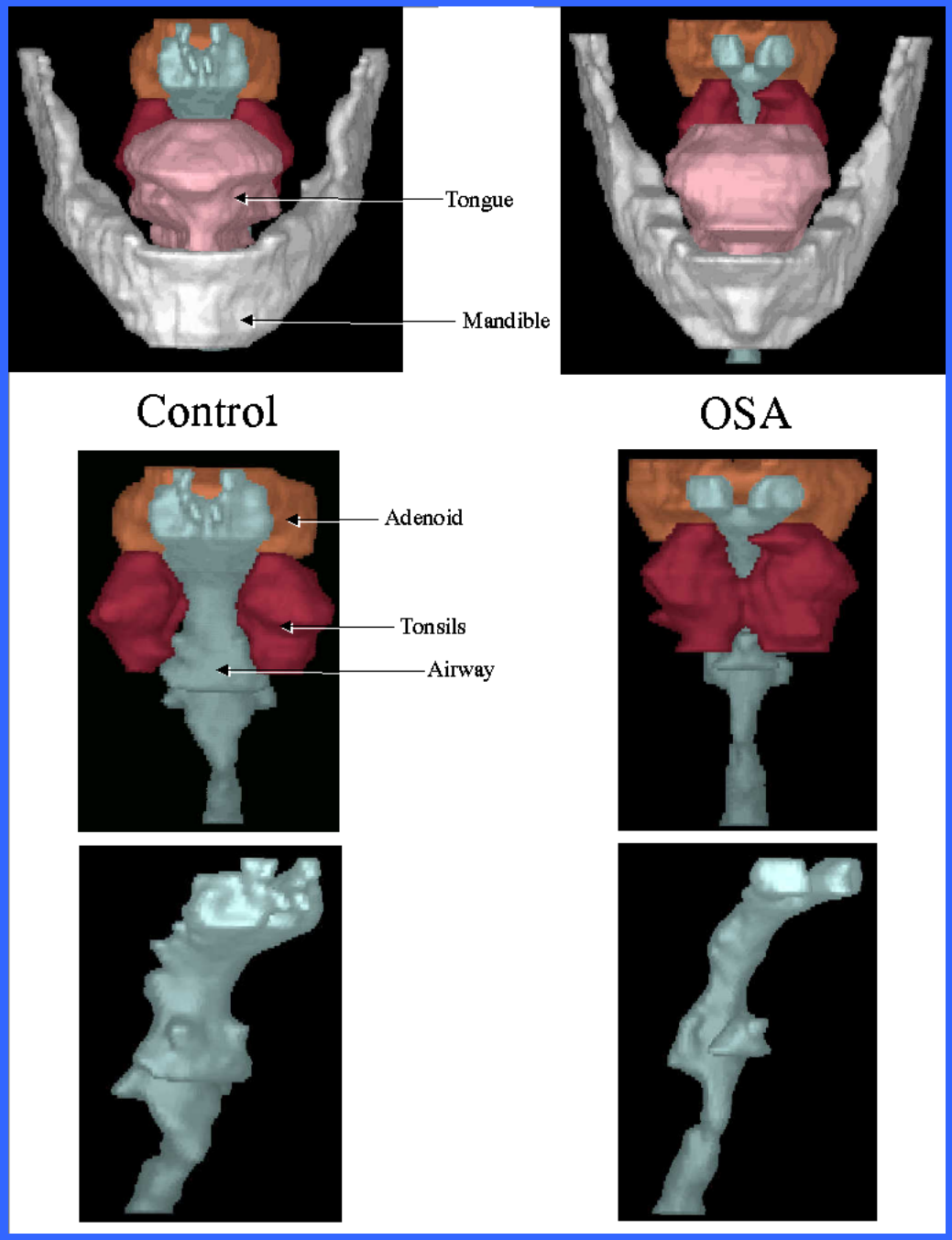
Tongue
Mandible
Control
OSA
Adenoid
Tonsils
Airway

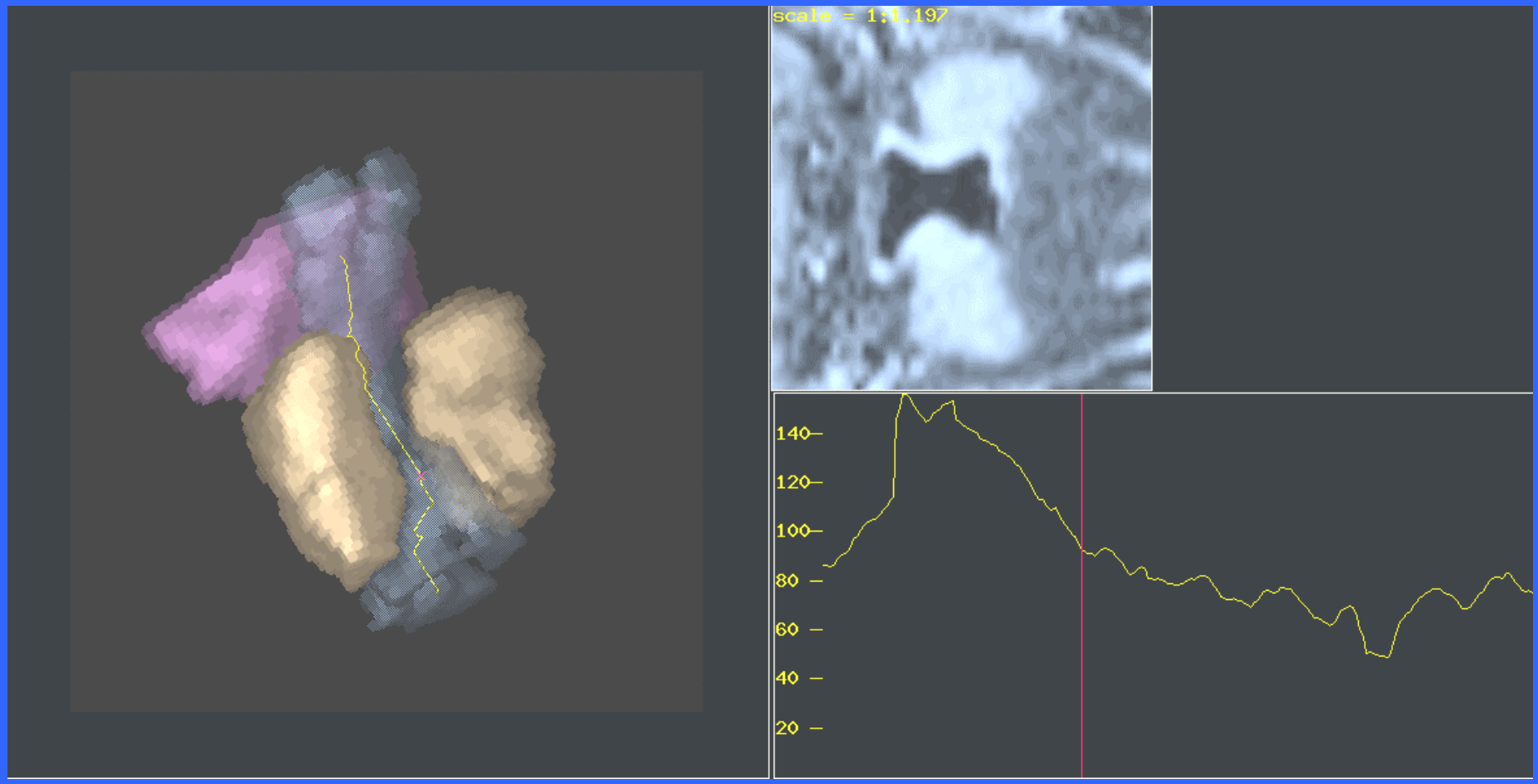

Left: A rendition of the airway (together with its central line) and the adenoid, tonsil, and palatine tonsil, all segmented from an MR image.

Right: A cross section orthogonal to the central line at a point on the central line (top) and the cross-sectional airway area as a function of distance along the central line (bottom).

8. CT Angiography

To clearly display the vascular tree free of other clutters, particularly bone, via CTA.

User interaction is minimal – specification of seed voxels in bone. Bone removal is then automatic.

Team: P.K. Saha, J.K. Udupa, J. Abrahams, P. LeRoux, and D. Leibeskind.

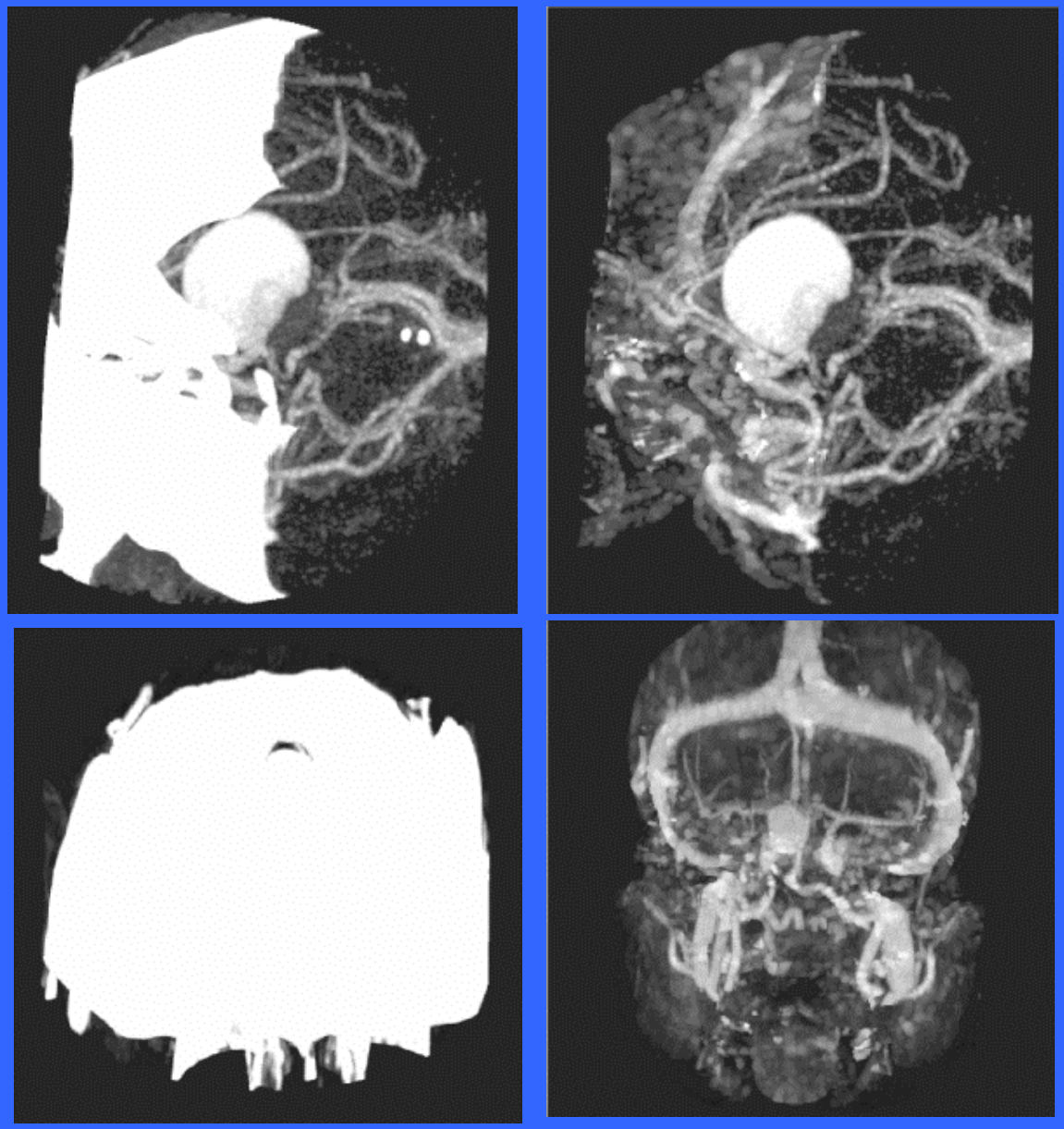

MIP renditions of cranial CTA without bone removal (left), after bone removal (right) for two studies.

9. Digital Topological Analysis of Trabecular Bone using *in vivo* Micro MRI

Digital topological analysis (DTA) is a method that allows unambiguous determination of the three-dimensional topology at each voxel location in a trabecular bone network. The analysis involves generation of a bone volume fraction map, which is subjected to sub-voxel processing to alleviate partial volume, blurring, followed by thresholding and skeletonization. The skeletonized images contain only surfaces, profiles, curves, and their mutual junctions as the remnants of trabecular plates and rods after skeletonization. DTA unambiguously classifies trabecular bone skeleton locations as belonging to plates, rods, or their mutual junctions using a complete 3D analysis of *in vivo* micro magnetic resonance images. Different DTA-based structural indices including what is termed an Erosion Index are computed. Recent studies have shown that DTA indices are the strongest discriminators of subjects with vertebral deformities from those without such deformities. These studies provided the first *in vivo* evidence for the structural implications inherent to postmenopausal osteoporosis accompanying bone loss.

Team: F.W. Wehrli, P.K. Saha, B.R. Gomberg, H.K. Song, and S.N. Wang.

more plate-like → more rod-like

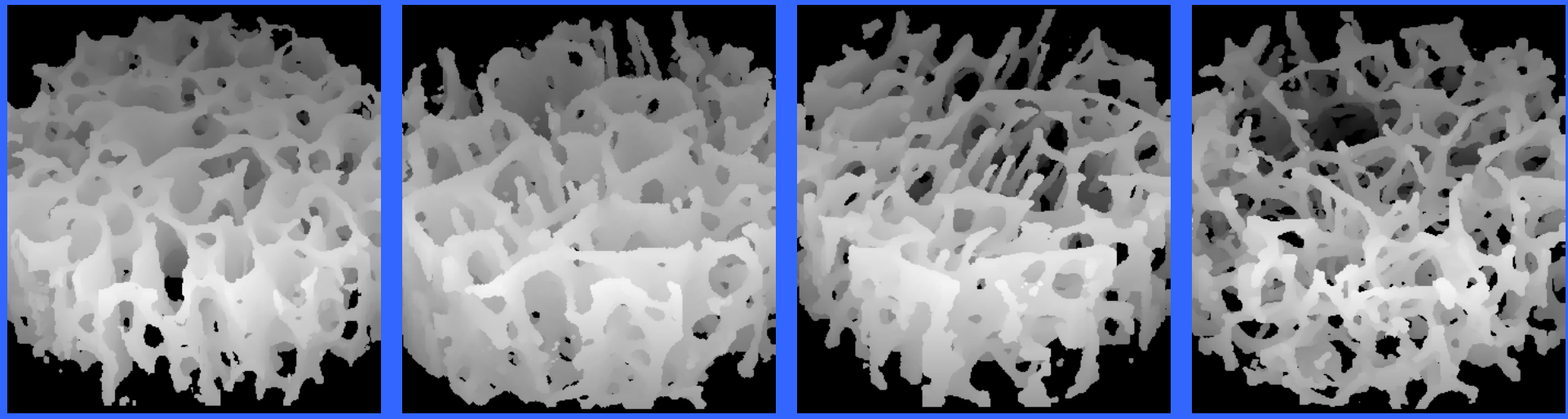

male, age 60 | female, age 68 | female, age 53 | female, age 74

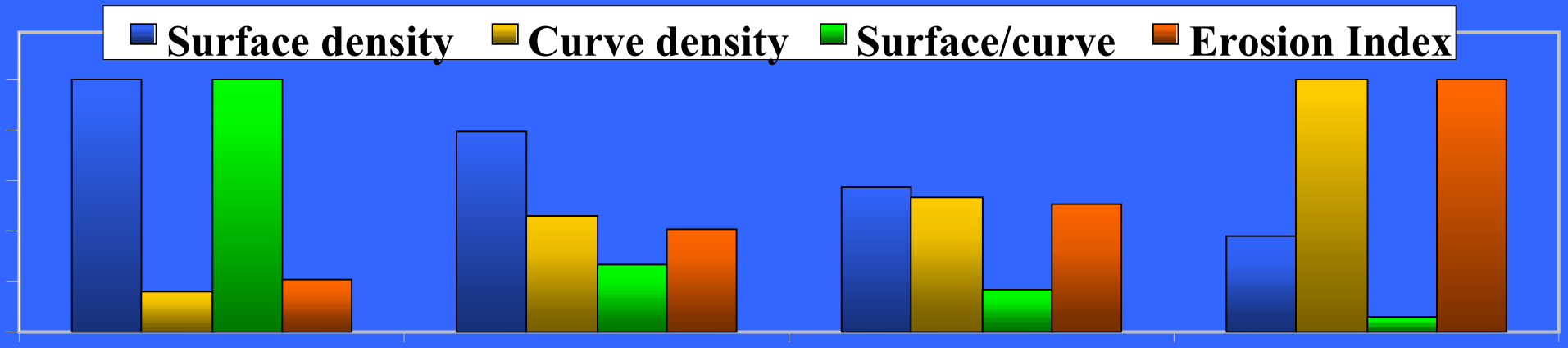

10. Lung Ventilation/Perfusion via MRI and CT

To quantitatively assess regional ventilation and perfusion in the lungs by using polarized helium MRI, fast CT, and MRI with Gadolinium. This project involves the segmentation of the lungs, the airway and the vessel tree in CT images and the airway and the vessel tree in MRI, the deformable registration of these entities and the computation of ventilation/perfusion parameters.

Team: R. Rizzi, J.K. Udupa, P.K. Saha, B. Wang, and J. Baumgarden.

(a)

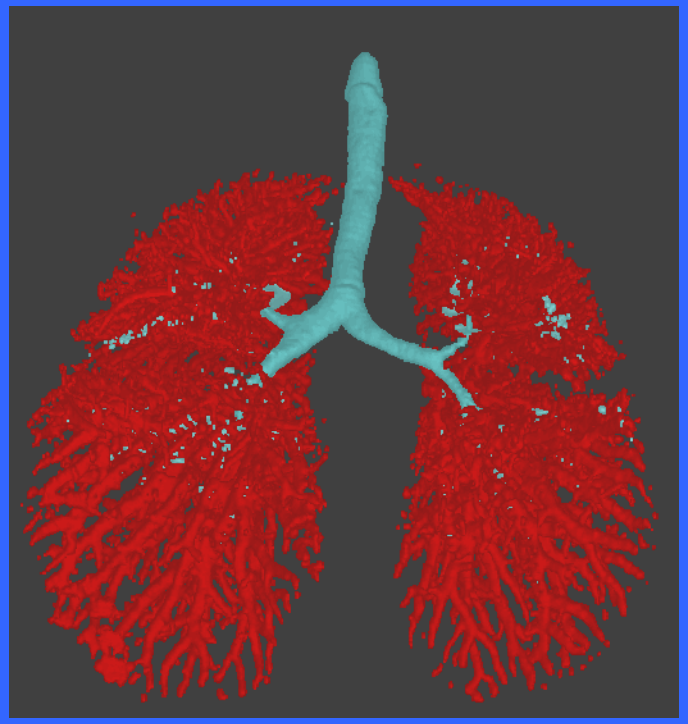

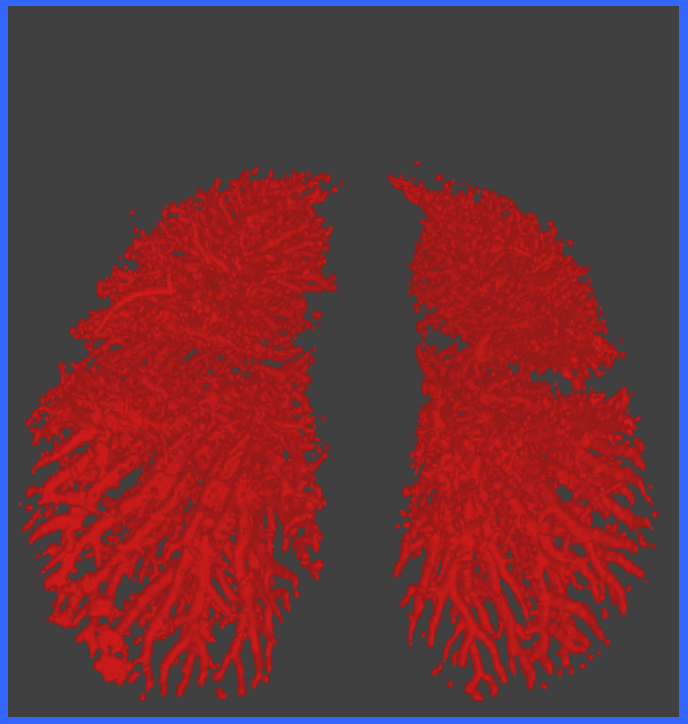

(b)

The vascular tree (b) and the airway tree and the vascular tree (a) segmented from a human lung – a 3D surface rendition.

(a)

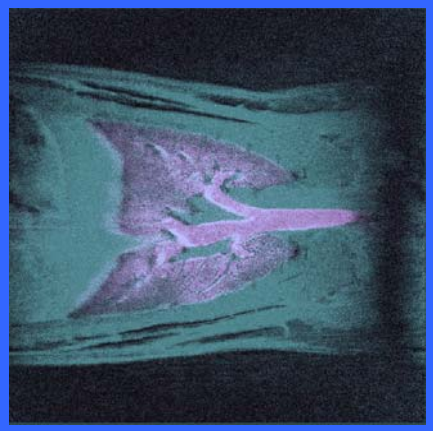

(b)

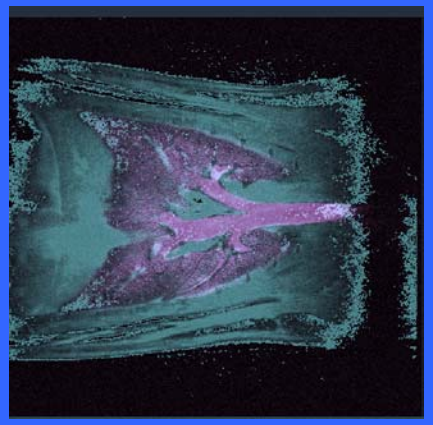

(c)

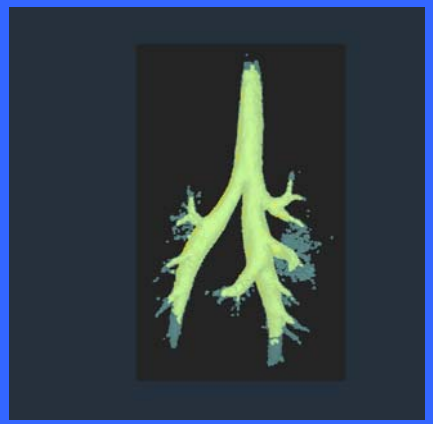

A Helium image of a pig's lungs (a); a registered helium and *PD* image super-imposed; (c) the airway tree segmented from Helium and *PD* image super-imposed in surface rendition.